ISSN 1063-7710, Acoustical Physics, 2018, Vol. 64, No. 6, pp. 665–672. © Pleiades Publishing, Ltd., 2018.

CLASSICAL PROBLEMS OF LINEAR ACOUSTICS AND WAVE THEORY

Effect of Sidewalls on Sound Transmission Loss Through Sonic Crystal[1]

P. Gulia[a], * and A. Gupta[a]

[a]*Acoustics and Vibration Laboratory, School of Engineering Indian Institute of Technology, Mandi, Himachal Pradesh, India*

**e-mail: preeti_gulia@students.iitmandi.ac*

Received December 13, 2017

Abstract—Sonic crystals are the periodic arrangements of scatterers embedded in a homogeneous material. Their ability to prevent sound wave to propagate in a particular range of frequency demonstrates their use as potential noise barriers. The sonic crystal considered in this work is an array of PVC cylinders (5 × 5) in air bounded by acrylic sheets. This paper studies the sound transmission loss in the sonic crystal by changing the location of the sidewalls. The optimized location of sidewalls of the sonic crystal to get wide band gap and high sound transmission loss has been investigated. To increase the transmission loss, a periodic structure having bi-periodicity, i.e., periodicity in two perpendicular directions is introduced. Both computational (Finite Element simulation) and experimental work has been performed to study the sound transmission loss and the band gaps. To bridge the gap between the two results, an improved finite element model has been proposed with an aim to replicate the experimental situation more closely. Generally, in experiments, insertion loss is calculated while numerically transmission loss is computed, and the two are compared. In this paper, a comparison between insertion loss and transmission loss has also been made numerically, which is compared with the experimental results.

Keywords: sonic crystal, sound-hard boundary, stopband, sound propagation, bi-periodicity

DOI: 10.1134/S1063771018060039

1. INTRODUCTION

Wave propagation over a periodic domain has been an area of growing interest of researchers from last few decades. Periodic structure implies the periodic arrangement of scatterers embedded in a homogeneous material. Periodic structures do not act the same with all frequencies of the wave. There are certain frequencies, which cannot propagate over periodic structure made of particular dimensions and materials. The usage of the periodic structure was initiated in 1887 by Lord Rayleigh [1]. He showed some stopbands for electromagnetic waves in one-dimensional periodic structure. Later in 1987, this idea was used by Eli Yablonovitch and Sajeev John [2, 3], which made the periodic structure a concerned area of research interest. Depending on the area of applications, these periodic structures are named differently such as sonic crystals, photonic crystals, and phononic crystals. When the periodic structures are made for the electromagnetic wave propagation, they are called photonic crystals. When the periodic structures are made for the sound wave propagation, they are called sonic crystals. This paper deals with the sound propagation over the periodic structure.

In 1995, Martinez et al. [4] were the first group of researchers who used a periodic structure subjected to the sound waves. They used a three-dimensional periodic sculpture, which was made by Eusebio Sempere in Madrid. This was a circular structure having a large outer domain. They measured the sound pressure across this structure in the outdoor area and it was found that the amplitude of the sound wave of frequency ranging from 1500 to 2000 Hz reduced significantly while propagating through this structure. This was a splendid finding in the area of acoustic wave propagation in the periodic structure and led to increasing diversion of research in this area.

There are various applications of the sonic crystals like frequency filter, sound diffusers, liquid sensors, acoustic diode, acoustic cloaking etc. However, sonic crystals are mainly known for noise barriers. A major problem associated with the sonic crystal is that it does not provide adequate transmission loss at a low filling fraction. Martinez et al. [5] demonstrated a periodic structure, in which a number of trees were arranged in a regular pattern like sonic crystal. The results showed a sound attenuation which was less than 10 dB obtained at a frequency lower than 500 Hz.

Band gaps in a periodic structure are originated as a result of Bragg's scattering, and location of the center

[1] The article is published in the original.

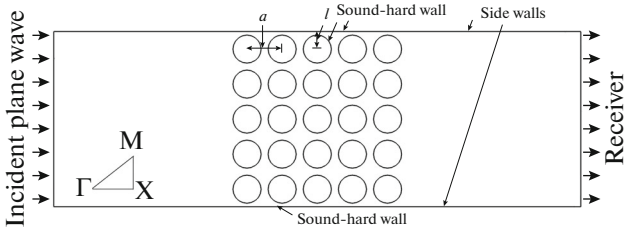

Fig. 1. A schematic diagram of a theoretical model of sonic crystal.

frequency of first band gap is calculated using Bragg's criteria [6]. Castineira et al. [7] presented an overlapping numerical model that enabled to split a 3D problem into 2D. They used absorbing materials and a resonant cavity in the scatterers to enhance transmission loss. Results satisfied the Bragg's criteria and gave a significant transmission loss. There are certain methods to calculate the band gap and dispersion properties of a periodic structure. Different types of propagating wave affect the dispersion properties of the structure. More information about the sound wave leads to less uncertainty in choosing the dispersion properties [8]. Zhao et al. [9] calculated the eigenmodes and band gaps of a three-component pillared phononic crystal plate using finite element method. They did a parametric study by varying the lattice constant, height and diameter of the pillars and developed a low-frequency vibration insulation in the plate structure. Morandi et al. [10] calculated the sound insulation and the reflection index over a sonic crystal. They did free field measurements to window out the diffraction effect of wave and calculated the band gap in a 1/3-octave band numerically and verified with the experimental results. Cai et al. [11] used Helmholtz resonators inside a periodic structure to increase the transmission loss. The results showed that the increasing the number of Helmholtz resonators increased the sound reduction performance of the periodic structure. Karabutov et al. [12] studied the transmission spectrum of a periodic structure consisting of solid layers in a liquid medium. It was found that wave propagation in opposite direction showed the interference nature with the directly propagating wave and transmission spectrum of a direct wave got changed with changing the parameters of the opposite pressure wave.

The frequency corresponding to the first peak of the sound transmission loss in a sonic crystal can be predicted using Bragg's criteria [13]. By increasing the filling friction and the diameter of scatterers, a sonic crystal shows a wider band gap and higher sound attenuation. A sonic crystal having filling fraction larger than 0.44 shows a complete band gap [14]. There are many parameters influencing the sound transmission loss in a sonic crystal, e.g. dimension of scatterers, their number, their material properties, the lattice constant, filling fraction, types of periodicity, and shape of scatterers etc., which have been studied by many authors [13–17]. However, the effect of the location of external walls on the sound transmission loss has not been studied previously.

In this work, the sound transmission loss is studied numerically as well as experimentally by changing the location of sidewalls in a sonic crystal. A bi-periodic structure is proposed and the effect of varying the lattice constant in the direction perpendicular to the direction of sound propagation is analyzed by an eigenfrequency study. The purpose of this work is to find out the suitable position of external sidewalls to get maximum sound attenuation. Finally, an improved theoretical model of the sonic crystal is proposed, for which results are found to be in a better match with the experimental results.

2. FINITE ELEMENT ANALYSIS

A schematic diagram of a 2D sonic crystal is shown in Fig. 1. There are total 25 scatterers arranged periodically in the middle of a rectangular domain (length 75 cm and width varying from 24.6 to 29 cm). The width of the sonic crystal is the distance between exterior sidewalls. The periodic distance between scatterers (*a)* is 5 cm and the radius of scatterers (*r*) is 2 cm. In material properties, PVC properties are given to the scatterers and air properties are given to the surrounding. The density of air is taken as 1.25 kg/m^3 and the sound speed in air is 343 m/s. The density of PVC is 1300 kg/m^3 and the sound speed in PVC is 1060 m/s.

A source of the plane wave is applied at the inlet of the sonic crystal. Plane wave radiation conditions are applied at the source and the receiver boundaries (left and right). A sound-hard boundary condition (i.e., the boundary, through which the sound cannot propagate) is applied at the scatterers and the exterior sidewalls of the sonic crystal (top and bottom). Particle velocity of the sound wave perpendicular to the sound-hard boundary is zero and sound waves are fully reflected after colliding with this boundary. Eq. (1) represents the sound-hard boundary condition. Due to the sound-hard property of scatterers, sound waves reflect repeatedly in the structure, which causes acoustic interference inside the sonic crystal. There are certain frequencies, which cannot propagate due to the destructive interference generated in the sonic crystal.

From the source boundary, forward traveling sound waves collide with the scatterers, and after reflecting from the scatterers, some of the waves travel back. However, at receiver boundary, it receives only the forward traveling waves. Eq. (2) and (3) show the

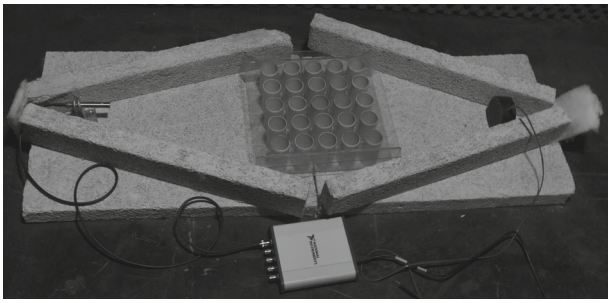

Fig. 2. Experimental setup after removing the top layer of the absorbing material.

boundary conditions applied at the inlet and the outlet respectively.

$$\left(-\frac{\nabla p}{\rho}\right)\mathbf{n} = 0, \tag{1}$$

$$\left(-\frac{\nabla p}{\rho}\right)\mathbf{n} = \frac{i\omega}{\rho c_c} p - \frac{i\omega}{\rho c_c} p_0, \tag{2}$$

$$\left(-\frac{\nabla p}{\rho}\right)\mathbf{n} = \frac{i\omega}{\rho c_c} p, \tag{3}$$

where p is the acoustic pressure, p_0 is the incident radiation pressure, $\mathbf{n}$ is the normal vector, $\mathbf{r}$ is the direction vector, $\mathbf{k}$ is the wave vector, ω is the angular frequency of the sound wave, ρ is density and c_c is the sound speed.

A COMSOL Multiphysics software is used for finite element analysis in the pressure acoustic frequency domain. For meshing, we did a convergence study and found that the solution converges when the maximum size of the element is taken as ten points per unit minimum wavelength shown in Fig. 3a. Triangular elements are created in the geometry after meshing with the maximum element size of 0.57 cm.

To calculate the sound transmission loss (T), we took an average sound power difference at the source and the receiver side. On the logarithmic scale, it can be represented by the following equation:

$$T = 10\log_{10}\left(\frac{w_{\text{in}}}{w_{\text{out}}}\right). \tag{4}$$

We calculated the transmission loss by changing the various positions of the sound-hard wall (parameter l in Fig. 1).

For the eigenfrequency analysis, the pressure acoustic eigenfrequency domain is used in COMSOL Multiphysics.

We apply the Bloch–Floquet periodicity conditions on the boundary of a unit cell and vary the wave vector over first Brillouin zone to calculate the complete band structure. The Bloch–Floquet theorem is applicable only for the periodic structure. Waves traveling in the sonic crystals are Bloch waves [18] and represented as:

$$p(x) = j(x)e^{ikx}, \tag{5}$$

where $\varphi(x)$ is a periodic function. In the sonic crystal, scatterers are arranged with a periodic distance a. So, the periodic function can be represented as:

$$\varphi(x) = \varphi(x + a). \tag{6}$$

Combining Eq. (4) and eq. (5), we get Bloch–Floquet equation (Eq. 7):

$$p(x + a) = \varphi(x)e^{ik(x+a)}. \tag{7}$$

In the first Brillouin zone, k_x varies from 0 to π/a, where k_y is 0 for the ΓX-direction, k_x is π/a and k_y varies from 0 to π/a for the XM-direction, and k_x and k_y both vary from 0 to π/a for the ΓM-direction [19]. The band gap, in which the sound cannot propagate in all these three directions, is called a full band gap.

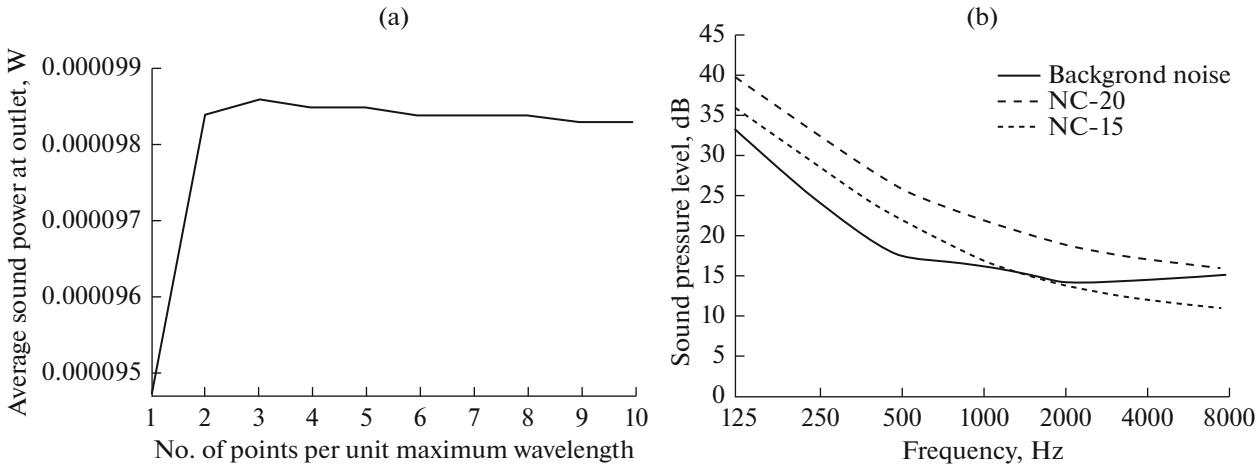

Fig. 3. (a) Convergence study, (b) background noise inside the acoustic enclosure.

3. EXPERIMENTAL SETUP

In the experimental setup, 25 PVC pipes are arranged periodically between two acrylic sheets (top and bottom). The diameter and height of PVC pipes are 4 and 7 cm respectively. Top and bottom faces of the sonic crystal are covered with acrylic sheets with dimensions 30 × 30 × 0.3 cm. The inlet and the outlet of the structure are open for the sound wave propagation. The remaining two sides are closed using acrylic sheets, which form the sidewalls of the periodic structure. The height of sidewalls is the same as the height of PVC pipes. Acrylic sheets (surface density 3.54 kg/m^2) act as sound-hard boundaries for the sonic crystal. To minimize the reflection, the experimental model is surrounded by the acoustic fibrette material (NRC ~ 1).

Figure 2 shows the complete experimental set-up after removing the upper layer of acoustic fibrette. This whole setup is kept inside an acoustic enclosure to nullify the effect of background noise. Background noise of acoustic enclosure is measured using the sound level meter CESVA SC310. The background noise of the enclosure lies between noise criteria NC-15 to NC-20 as shown in Fig. 3b. Noise criteria (NC) curves are used to describe the background noise. An NC curve sets a standard for the background noise. For various locations like sound broadcasting, recording studios, concert and recital halls, it falls under NC-15 to NC-20. In the acoustic enclosure, the maximum background noise at 125 Hz is 33.4 dB. A minimum sound pressure level inside the acoustic enclosure after the sound attenuation through the sonic crystal is 47 dB, which is 10 dB higher than the maximum background noise level. So, the effect of background noise on the measurement is considered to be negligible.

A Logitech speaker of diameter 7 cm is used as a sound source. A ½" GRAS free-field response microphone with National Instrument NI-4432 is used to measure the sound pressure. The distance between the speaker and the inlet boundary of the structure is 30 cm. The distance between the outlet boundary of the sonic crystal and the microphone is also 30 cm. The sound incident from the speaker is averaged ten times. The sound attenuation is measured in the form of insertion loss. The experiments are done with and without the sonic crystal, and the difference between the two sound pressure levels gives the sound insertion loss.

4. EXPERIMENTAL AND THEORETICAL RESULTS

In this section, we will discuss the effect of the location of sidewalls on the band gap and the sound transmission loss. We did a finite element calculation on a sonic crystal with various positions of sidewalls. Figure 4a represents the sound transmission loss *vs.* frequency for the sonic crystal. The results show that transmission loss is highest when the sound-hard boundary is present at a distance which is half of the periodic constant from the center of end scatterers i.e. $l = a/2$. Sound-hard wall positioned below 2.5 cm and above 2.5 cm from the center of end scatterers result in low transmission loss.

In the sonic crystal, every middle line between the two scatterers parallel to the direction of propagation of wave will act as a sound-hard boundary, and sound cannot propagate through this boundary due to symmetricity. Therefore, sidewalls of the sonic crystal must be at the distance $a/2$ from the center of end scatterers to get maximum transmission loss. Placing the sidewalls at a different position only affects the magnitude of transmission loss, but location and width of the band gap remain the same as shown in Fig. 4a.

Figures 4b, 4c, 4d show the experimental validation of the finite element results at $l = 4.5$, 2.5 and 2.2 cm respectively. l is the distance between the center of end scatterers and sidewall. It is found from the results that sound attenuation is higher when the sound-hard wall is present at 2.5 cm ($a/2$) from the center of end scatterers.

Sound attenuation in experiments is calculated in the form of insertion loss. In all three cases, there is a sudden hike in the insertion loss in the lower frequency region (below 1900 Hz), which is not present in the theoretical results. Then, the band gap appears between 1900 to 4700 Hz and shows a good amount of insertion loss. Sonic crystal shows a clear dome shape curve when location of the sidewall is 2.5 cm, and the maximum sound insertion loss in this band gap is 30 dB. When the sidewalls are located at 4.5 cm, the maximum sound insertion loss is 12 dB. In the third case, when sidewalls are present at 2.2 cm, we got an irregular shape of the curve in this region and the maximum insertion loss is 28 dB. In the experimental result, the band gap matches well with the finite element predictions, but transmission loss obtained in finite element simulation is higher than the results obtained in experiments. To bridge the gap between the two results, an improved finite element model has been proposed in section 5 to replicate the experimental situation in a more realistic way.

Figure 5a shows the transmission loss of a bi-periodic structure versus a mono-periodic structure. A bi-periodic structure means the structure has periodicity in two directions. In a mono-periodic structure, the lattice constant is the same in both x and y directions, i.e. $a_x = a_y = 5$ cm. In a bi-periodic structure, lattice constants are different in x and y directions, i.e. $a_x = 5$ cm, $a_y = 4.6$ cm. The radius of scatterers is 2 cm in both cases. Totally, twenty-five scatterers (5 × 5) are present periodically with periodicity a_x in the x-direction and a_y in the y-direction. The filling fraction in the bi-periodic structure (0.546) is higher than in the mono-

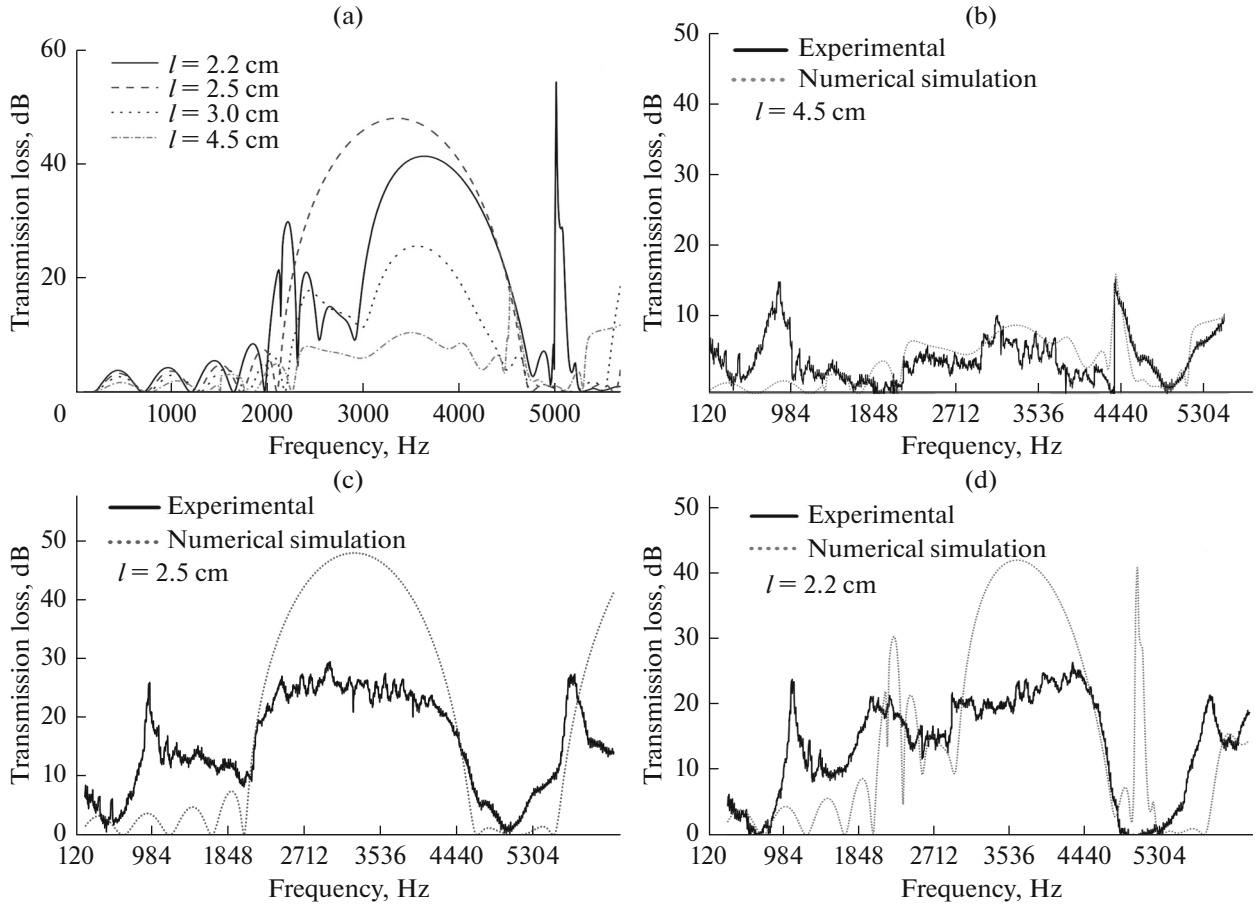

Fig. 4. (a) Sound transmission loss in a sonic crystal with respect to different positions of sidewalls calculated using FEM, (b) theoretical vs. experimental at $l = 4.5$, (c) $l = 2.5$ and (d) $l = 2.2$ cm.

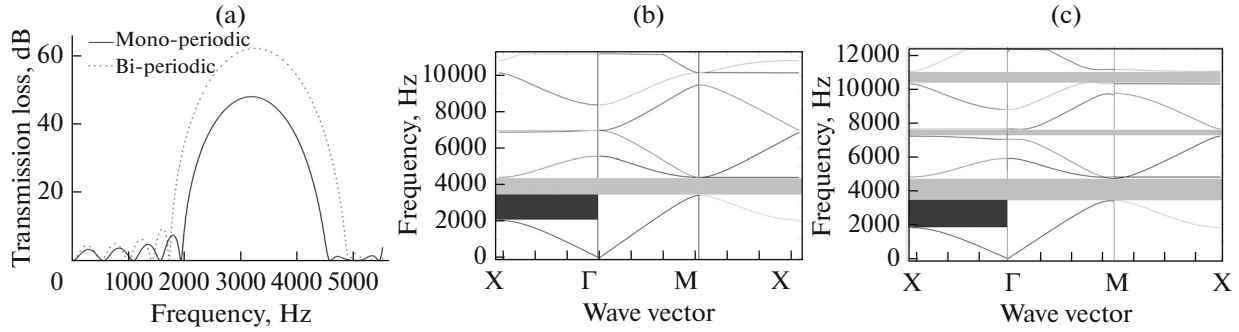

Fig. 5. FEM simulation results: (a) transmission loss in a mono-periodic vs. bi-periodic sonic crystal, (b) complete band structure in a mono-periodic and (c) a bi-periodic sonic crystals.

periodic structure (0.503). This is a good way of increasing the filling fraction by introducing periodicity in two directions. Increase in filling fraction leads to higher sound insulation. Figure 5a shows sound transmission loss and the band gap of bi-periodic and mono-periodic structures when sound waves propagate in the ΓX region. We found that sound transmission loss and the bandwidth both are greater in the bi-periodic than in the mono-periodic structure.

We did an eigenfrequency analysis using Bloch-Floquet periodicity on the unit cell for two sonic crystals having different directional periodicity but same material properties. Figures 5b, 5c show the band structure of two sonic crystals: (i) the structure is

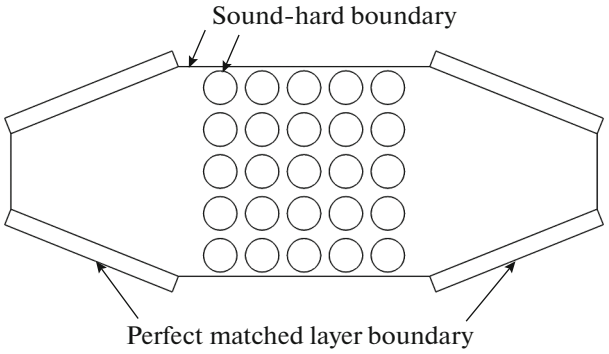

Fig. 6. A schematic diagram of the improved theoretical model of a sonic crystal.

mono-periodic, i.e. $a_x = a_y = 5$ cm, and the radius of scatterers is 2 cm, (ii) structure is bi-periodic, i.e. $a_x = 5$ cm; $a_y = 4.6$ cm, and the radius of scatterers is 2 cm. We calculated the eigenfrequencies as functions of the wave vector.

Figures 5b, 5c show six eigenmodes in the frequency range from 0 to 12000 Hz. The results show a complete band gap in both periodic structures. However, the structures differ at the position of the opening of the stopband. In Fig. 5c, the first full band gap starts at 3400 and ends at 4800 Hz. In Fig. 5b, the first full band gap starts at 3500 and ends at 4400 Hz. For the second case, the bandwidth is larger than for the first case.

In a full band gap, sound waves cannot propagate in any direction (ΧΓΜΧ). However, the band gap in the ΓΧ region blocks the sound wave only in the x-direction. For the first case, the band gap in the ΓΧ region starts at 2000 and ends at 4400 Hz. For the second case, the band gap in the ΓΧ region starts at 1800 and ends at 4800 Hz. The sonic crystal shows a wide band gap of 2200 Hz in the first case and 3000 Hz in the second case in the ΓΧ region. However, in the case of bi-periodicity, the sonic crystal shows three full band gaps below 12000 Hz, while the mono-periodic structure shows only one full band gap. The bandwidth of the first full band gap is larger in the bi-periodic sonic crystal than in the mono-periodic one. The bandwidth of the second and third full band gaps in the bi-periodic structure are 600 and 750 Hz respectively. The results show that decreasing the lattice constant in the y-direction not only increase sound transmission loss and bandwidth but also increase the number of band gaps.

5. IMPROVED THEORETICAL MODEL

In the previous section, sound attenuation is calculated by changing the location of sidewalls theoretically as well as experimentally, and results are in good agreement. In the experimental results, the band gap matches well with the finite element results but there are some differences in the transmission loss obtained in finite element simulation and experiments, as seen in Fig. 4. There are some possible reasons for the differences between these two results. First, the geometry for finite element simulation is quite idealistic, while in experiments, the geometry is somewhat different. Second, in the theoretical model, we have an incident plane wave on the inlet of the sonic crystal. However, in the experimental model, some non-planar wave is also present due to speaker profile and reflections in the setup. Third, in the experimental model, PVC scatterers are surrounded by four thin acrylic sheets. During the sound propagation over the experimental model, there may be vibration generation in the acrylic sheets. In the theoretical model, sound-hard properties are given to the acrylic sheets, which may lead to some differences. Fourth, we measured the sound insertion loss experimentally while numerically we calculated the sound transmission loss. Generally in literature, [7] researchers do not differentiate between transmission loss and insertion loss; however, we have calculated these two results separately for the improved theoretical model.

The previous theoretical model is a very idealistic one, in which a plane wave directly strikes to the sonic crystal. But it is quite difficult to achieve the plane wave practically. To obtain the plane wave in the experimental model, vertical inclined walls of acoustic fibrette are used around the front and the rear end of the experimental set-up, so that it can absorb the diverging sound waves and minimize the reflections from the surrounding environments and sound originated from the speaker can directly reach to the sonic crystal. But every absorbing material has its own properties of the sound absorption, which is also a function of frequency. This causes some discrepancy between the theoretical and the experimental results shown in Fig. 4. So, we tried to improve the theoretical model by introducing the boundary condition of a sound absorbing layer around the rear and the front end of the model.

We focused on the ideal case of the sonic crystal in which sidewalls are present at 2.5 cm ($a/2$) from the center of end scatterers and tried to make a more realistic theoretical model with the experimental setup. To obtain a more exact theoretical model, inclined perfectly matched layers (PML) are used as a boundary condition to simulate this problem, and sound insertion loss is calculated by the logarithmic difference of the sound power at outlet with and without a sonic crystal. The rest of the details is the same. PML is an artificial sound absorbing layer, which is used as a boundary condition to solve numerical problems. A schematic diagram of the improved theoretical model of the sonic crystal is shown in Fig. 6.

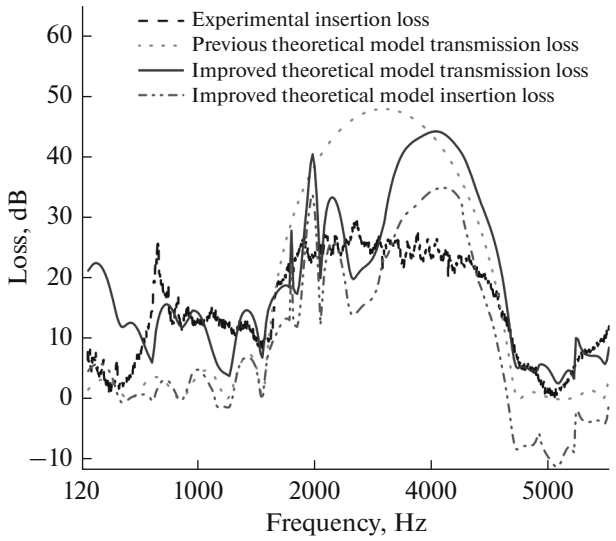

Fig. 7. Transmission loss vs. insertion loss in the experimental and theoretical models when sidewalls are present at 2.5 cm.

In this case, we calculated transmission loss as well as insertion loss and compared with the experimental and the previous theoretical model results shown in Fig. 7. The band gap location is same in all the cases, but average transmission loss in the improved theoretical model is less than the transmission loss in the previous model due to insertion of PML boundary condition. The maximum transmission loss in the previous theoretical model is 48 dB, whereas the average transmission loss in the improved model has significantly reduced and shows a maximum value of 44 dB in this region. Insertion loss in the improved theoretical model is quite comparable with the experimental insertion loss. The maximum insertion loss in the improved model is 35 dB. The proposed improved model has a better physical correlation with the experimental setup, and therefore the results are in better agreement compared to the simplistic finite element model.

6. CONCLUSIONS

In this work, the effects of sidewalls and bi-periodicity in the sonic crystals have been studied. Location of the band gap and sound transmission loss is measured corresponding to the different locations of the sound-hard sidewalls. The results show that an outer wall of the sonic crystal situated at a distance of half of the periodic distance from the center of end scatterers is the best to give wide band gap and high transmission loss. To improve the transmission loss, bi-periodicity is incorporated in the structure by reducing the lattice constant in the y-direction. When the result of the bi-periodic structure is compared with the mono-periodic structure, it is found that the bi-periodic structure shows higher transmission loss than the mono-periodic structure with an increased number of band gaps. Therefore, it is concluded that exterior sidewalls of a sonic crystal should be at the distance $a_y/2$ from the center of end scatterer to get maximum transmission loss; here a_y is the lattice constant in the y-direction. Two periodic structures having similar material properties but a different type of periodicity, show different bandwidth and sound transmission loss. This property can be used as per the requirement of the incoming noise frequency component and the space considerations. An improved theoretical model, which shows better interpretation correlating with the experiment, is also simulated. Insertion loss predicted by the new theoretical model is in better agreement with the insertion loss found in the experiments. In the future, boundary conditions can be improved by incorporating the impedance boundary for the PML, which matches with the impedance of acoustic fibrette.

ACKNOWLEDGMENTS

The authors would like to acknowledge the facility of Acoustics and Vibration Lab. provided by Indian Institute of Technology Mandi for carrying out this work. The authors would also like to acknowledge the assistance provided by SERB (Science and Engineering Research Board) through the DST project YSS/2015/001245.

REFERENCES

1. Lord Rayleigh, Philos. Mag. J. Sci. **24** (147), 145 (1887). http://dx.doi.org/. doi 10.1080/14786448708628074
2. E. Yablonovitch, Phys. Rev. Lett. **58** (20), 2059 (1987). https://doi.org/10.1103/PhysRevLett.58.2059.
3. S. John, Phys. Rev. Lett. **58** (23), 2486 (1987). https://doi.org/10.1103/PhysRevLett.58.2486.
4. R. Martinez-Sala, J. Sancho, J. V. Sanchez, V. Gomez, J. Llinares, and F. Meseguer, Nature **378** (6554), 241 (1995). https://doi.org/10.1038/378241a0.
5. R. Martinez-Sala and J. V. Sanchez, J. Sound Vib. **291**, 100 (2006). https://doi.org/10.1016/j.jsv.2005.05.030.
6. Y. Pennec, J. O. Vasseur, B. Djafari-Rouhani, L. Dobrzynski, and P. A. Deymier, Surf. Sci. Rep. **65** (8), 229 (2010). https://doi.org/10.1016/j.surfrep.2010.08.002.
7. S. Castineira-Ibanez, C. Rubio, and J. V. Sanchez-Perez, Build. Environ. **93**, 179 (2015). https://doi.org/10.1016/j.buildenv.2015.07.002.
8. Yu. Bobrovnitskii, Acoust. Phys. **57** (4), 442 (2011). https://doi.org/10.1134/S1063771011040026.
9. H. Zhao, H. Guo, M. Gao, R. Liu, and Z. Deng, J. Appl. Phys. **119** (1), 1 (2016). http://dx.doi.org/. doi 10.1063/1.4939484

10. F. Morandi, M. Miniaci, A. Marzani, L. Barbaresi, and M. Garai, Appl. Acoust. **114**, 294 (2016). https://doi.org/10.1016/j.apacoust.2016.07.028.
11. C. Cai, C. Ming, and X. Wang, Appl. Acoust. **122**, 8 (2017). https://doi.org/10.1016/j.apacoust.2017.02.006.
12. A. Karabutov, V. Kozhushko, I. Pelivanov, and G. Mityurich, Acoust. Phys. **47** (6), 721 (2001). https://doi.org/10.1134/1.1418900.
13. G. Jiang, Y. Liu, Y. Wu, W. Xu, Q. Kong, and C. Zhang, Appl. Acoust. **116**, 117 (2017). https://doi.org/10.1016/j.apacoust.2016.09.020.
14. T. Miyashita, Jpn. J. Appl. Phys. **41** (5), 3170 (2002).
15. D. Torrent, J. Sanchez Dehesa, and F. Cervera, Phys. Rev. B **75**, 241404 (2007).
16. S. Yang, W. Yu, and N. Pan, Phys. B (Amsterdam, Neth.) **406** (4), 963 (2011).
17. L. Zhong, F. Wu, X. Zhang, H. Zhong, and S. Zhong, Phys. Lett. A **339**, 164 (2005).
18. A. Gupta, Acoust. Phys. **60** (2), 223 (2014). https://doi.org/10.1134/S1063771014020080.
19. D. P. Elford, L. Chalmers, F. Kusmartsev, and G. M. Swallowe, J. Acoust. Soc. Am. **130** (5), 1 (2011). https://doi.org/10.1121/1.3643818.